Photophysical Characterization of Fluorescent DNA Base Analogue, tC

L. Marcus Wilhelmsson,* Peter Sandin, Anders Holmén,† Bo Albinsson, Per Lincoln, and Bengt Nordén

Physical Chemistry Section at the Department of Chemistry and Bioscience, Chalmers University of Technology, SE-41296 Gothenburg, Sweden, and Physical Chemistry, Discovery Bioanalytical Chemistry & Technologies, AstraZeneca R&D Mölndal, S-43183 Mölndal, Sweden.

Received: April 8, 2003; In Final Form: June 11, 2003

The novel fluorescent DNA cytosine base analogue 1,3-diaza-2-oxophenothiazine, tC, has previously been shown to have a remarkably preserved high quantum yield upon incorporation into a single strand of peptide nucleic acid, PNA, as well as when the latter is hybridized with a complementary DNA to form a PNA−DNA duplex. Here, we investigate fundamental photophysical properties of tC. Using fluorescence anisotropy, stretched film linear dichroism, and quantum chemical calculations, the transition moment polarizations of the lowest lying electronic states are determined. The neutral, base-pairing form of tC, having a fluorescence quantum yield of 0.2, is found to be the totally predominant species in a wide pH interval, 4−12. We show that the absorption band of tC at lowest energy, centered at 26 700 cm^{-1} and well separated from the nucleobase absorption, is due to a single electronic transition polarized approximately at 35° from the long axis of the molecule. The 2-deoxyribonucleoside of 1,3-diaza-2-oxophenothiazine, synthesized for further incorporation into DNA, was found to display a fluorescence quantum yield nearly the same as in the form of tC that was incorporated into PNA, confirming the notion of the tC nucleoside being a probe with very promising fluorescence properties essentially invariant of environment, also upon incorporation into a DNA strand and upon hybridization.

Introduction

Fluorescent DNA base analogues are of great interest as sensitive probes for detecting nucleic acids and studying the structure, dynamics, and interactions within nucleic acids as well as interaction between nucleic acids and other molecules (for recent review see Rist and Marino).[1] A great advantage with the fluorescent base analogues is that their size and structure enable them to be incorporated site-specifically into nucleic acid contexts with minimal disturbance of the native structure, as compared to fluorescent dyes, covalently linked to the backbone of the oligonucleotide. Two essential properties of fluorescent base analogues are their ability to form specific base pairs with the naturally occurring bases and to have a sufficient fluorescent quantum yield also after incorporation into nucleic acid systems. The most utilized fluorescent base analogue, 2-aminopurine (2-AP),[2,3] forms stable base pairs with thymine, but can also form moderately stable base pairs with cytosine.[4] Another disadvantage is the fact that the high intrinsic fluorescence quantum yield of 2-AP (68%) is reduced approximately 100-fold when incorporated into oligonucleotides.[2] The quantum yield of 2-AP is less sensitive to base pairing and hydrogen-bonding interactions, but sensitive to local and global conformational changes, which has been explained by stacking interaction with and collisional quenching by neighboring bases.[2,5] 2-AP has been used for probing structural and dynamic changes in damaged or mismatched DNA,[6,7] and in interactions between DNA and, for example, polymerases,[8−12] restriction endonucleases,[13−15] and repair enzymes.[16−19] However, the sensitivity of its excited-state lifetimes to environment makes it rather unreliable as a probe of molecular dynamics using fluorescence anisotropy measurements and energy transfer.

A recently developed group of fluorescent base analogues are the pteridines (for a recent review, see Hawkins).[20] Of the available pteridines, the two guanine analogues 3-methylisoxanthopterine (3-MI) and 6-methylisoxanthopterine (6-MI) have been synthesized as phosphoramidites and incorporated into DNA oligonucleotides.[21−24] Like 2-AP, these probes have high fluorescent quantum yields in their free form, 88 and 70% respectively,[22] but exhibit a substantial reduction in quantum yields, up to 25-fold, upon incorporation into oligonucleotides. Another new group of fluorescent base analogues with promising properties is the benzoquinazolines,[25−27] which were originally designed to increase the stability of triple helices. Interestingly, they display high fluorescence quantum yield, both free and when included in oligonucleotide duplexes.[25] Although these base analogues are quenched when a third strand anneals to the duplex, they might have potential in selective detection of triplexes over duplexes.

In a different approach for developing fluorescent base analogues, Kool and colleagues have synthesized nucleotides containing aromatic polycyclic hydrocarbons, for example, pyrene and phenanthrene, in the place of the base.[28−31] These fluorescent base analogues obviously lack the hydrogen bonding specificity, but can sterically mimic a base pair, causing only relatively modest perturbations to the natural DNA helix, when incorporated against an abasic site.

Recently we reported on the interesting fluorescent properties of a novel fluorescent base analogue, 1,3-diaza-2-oxophenothiazine,[32] tC (Figure 1).[33] Previously it had been shown that this tricyclic cytosine analogue discriminates well between G and A targets[34] and also increases the base stacking, thus increasing the melting temperature of DNA−RNA−,[34] DNA−peptide

* Telephone: +46-(0)31-7723051. Fax: +46-(0)31-7723858. E-mail: mawi@phc.chalmers.se.

† AstraZeneca.

10.1021/jp034930r CCC: $25.00
Published on Web 07/29/2003

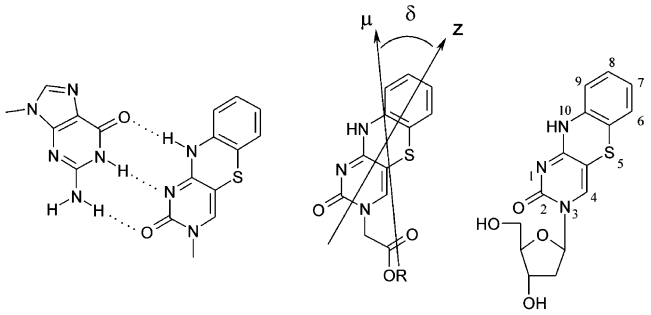

Figure 1. Structure of G−tC base pair on the left, tC nucleoside on the right, and derivatives of tC used in the measurements in the middle (R = H, CH_3, and K in 1,3-diaza-2-oxophenothiazin-3-yl acetic acid (AtC), its methyl ester (MtC), and its potassium salt (KtC), respectively). δ is an in-plane angle relative the molecule fixed reference axis parallel to the long axis of the molecule (z). Also included is the polarization of the lowest energy transition moment of tC (μ).

nucleic acid (PNA)−,[35] and PNA−PNA duplexes.[35] We have shown that the fluorescence quantum yield of tC is high (20%) and essentially the same whether incorporated into a PNA single strand (22%) or a PNA−DNA duplex (21%).[33] Like the fluorescent base analogues mentioned above, tC has an absorption band at 375 nm (26 700 cm^{-1}) well separated from the normal DNA band at 260 nm (38 500 cm^{-1}) and can, therefore, be selectively excited. Furthermore, we have shown that tC can serve as an excellent fluorescence resonance energy transfer (FRET) donor in a pair with rhodamine as acceptor.[33] In contrast to most earlier studies, where random orientation of donor and acceptor often has been assumed due to lack of reliable orientational information, the rigid and well-defined geometry of tC stacked within a duplex combined with its fluorescent properties could be a major advantage in FRET experiments for quantitative, accurate measurements of distances within molecular systems, provided transition moment data is accessible.

We here report an experimental and theoretical study on the photophysical properties of tC, with effects of solvents and pH. In particular, we determine the polarizations of the transition moment of the lowest lying electronic states of the neutral base-pairing form of tC using fluorescence anisotropy, stretched film linear dichroism, and quantum chemical calculations.

Materials and Methods

Chemicals. The tC derivatives of 1,3-diaza-2-oxophenothiazin-3-yl acetic acid (AtC) were synthesized from the methyl ester, which was obtained by alkylation of the anion of 1,3-diaza-2-oxophenothiazine (Roth et al.)[36] with methylbromoacetate, following the general procedure of Eldrup et al.[35] The 2-deoxyribonucleoside of 1,3-diaza-2-oxophenothiazine was synthesized according to Matteucci et al.[34] The buffers used for pH 4.0, 7.5, and 10 were sodium citrate, sodium phosphate, and glycine−NaOH at a total sodium concentration of 50 mM, respectively. Poly(vinyl alcohol) (PVA) was obtained as powder from E. I. du Pont de Nemours Co. (Elvanol). The organic solvents used were of spectrophotometric grade.

Film Preparation. A 12.5% (w/w) solution of PVA was prepared by dissolving PVA in water under heating to 100 °C. Portions of 5 mL were mixed with 3 mL of water solutions of the potassium salt of 1,3-diaza-2-oxophenothiazin-3-yl acetic acid (KtC), each containing ~0.2 mg of substance. The mixtures were poured onto horizontal glass plates and left to dry in a dust-free environment for more than 48 h, after which the films were removed from the plates and mechanically stretched 4 times their original length under the hot air from a hairdryer.

Extinction Coefficient Determination. The extinction coefficients of the methyl ester of 1,3-diaza-2-oxophenothiazin-3-yl acetic acid (MtC) in different solvents were determined using a 30-times dilution of a THF stock solution. The extinction coefficient was measured using a Varian Cary 4B spectrophotometer.

Fluorescence Measurements. The fluorescence quantum yields of the different derivatives of tC were determined relative to the quantum yield of 9,10-diphenylanthracene in ethanol (ϕ_f = 0.95).[37] The measurements were performed on a SPEX fluorolog τ-3 spectrofluorimeter (JY Horiba) between 25 000 and 13 500 cm^{-1} using an excitation wavenumber of 26 700 cm^{-1}.

The fluorescence excitation anisotropy spectra of KtC were measured on a SPEX fluorolog τ-2 spectrofluorimeter (JY Horiba) with the samples in H_2O/1,2-etandiol (1:2 mixture) glass at −100 °C, with Glan polarizers both on the excitation and emission beams. The excitation spectra were recorded from 41 700 to 22 200 cm^{-1}, and the emission was set at the fluorescence maximum, 19 800 cm^{-1}. The fluorescence anisotropy (r) was calculated as[38]

$$r(\tilde{\nu}_{exc}) = \frac{I_{vv}(\tilde{\nu}_{exc}) - I_{vh}(\tilde{\nu}_{exc})G}{I_{vv}(\tilde{\nu}_{exc}) + 2I_{vh}(\tilde{\nu}_{exc})G} \quad (1)$$

where I_{vh} refers to excitation spectrum recorded with the excitation polarizer in the *v*ertical and the emission polarizer in the *h*orizontal position, and so forth, and G is the ratio I_{hv}/I_{hh} used for instrumental correction. For an immobile chromophore with an electronic transition (i), the limiting anisotropy is related to the angle α_i between the absorbing and emitting transition moments according to

$$r_{0i} = \frac{1}{5}(3\cos^2\alpha_i - 1) \quad (2)$$

Hence, the anisotropy over a single isolated electronic transition will be constant, whereas in regions of the spectrum where electronic transitions overlap, it will show a wavenumber dependence according to

$$r_0(\tilde{\nu}_{exc}) = \frac{\sum_i \epsilon_i(\tilde{\nu}_{exc}) r_{0i}}{\sum_i \epsilon_i(\tilde{\nu}_{exc})} \quad (3)$$

with $\epsilon_i(\tilde{\nu}_{exc})$ being the molar absorptivity of transition i.

Linear Dichroism (LD) Measurements. Linear dichroism (LD) measurements were performed in stretched PVA matrices using a Varian Cary 4B spectrophotometer equipped with Glan air-space calcite polarizers in both sample and reference beams. LD is defined as

$$LD(\tilde{\nu}) = A_{II}(\tilde{\nu}) - A_{\perp}(\tilde{\nu}) \quad (4)$$

where $A_{II}(\tilde{\nu})$ and $A_{\perp}(\tilde{\nu})$ are the absorption of light polarized parallel and perpendicular to the macroscopic orientation axis (film stretching direction), respectively. The reduced linear dichroism of a uniaxial sample is defined as

$$LD^r(\tilde{\nu}) = \frac{A_{II}(\tilde{\nu}) - A_{\perp}(\tilde{\nu})}{A_{iso}(\tilde{\nu})} = 3\left(\frac{A_{II}(\tilde{\nu}) - A_{\perp}(\tilde{\nu})}{A_{II}(\tilde{\nu}) + 2A_{\perp}(\tilde{\nu})}\right) \quad (5)$$

where A_{iso} is the absorption of the corresponding isotropic sample. In a similar way as for the anisotropy mentioned above,

the LD^r of overlapping transitions can be calculated as

$$LD^r(\tilde{\nu}) = \frac{\sum_i \epsilon_i(\tilde{\nu}) LD_i^r}{\sum_i \epsilon_i(\tilde{\nu})} \quad (6)$$

The dichroism for a pure electronic transition, LD_i^r, for a molecule that has a rodlike orientation in a stretched PVA matrix is given by

$$LD_i^r = 3S_{zz}\left(\frac{3\cos^2\theta_i - 1}{2}\right) \quad (7)$$

where θ_i is the angle between the molecular orientation direction and the *i*th transition moment, and S_{zz} is the Saupe orientation parameter for the principal orientation axis, *z*.

Magnetic Circular Dichroism (MCD) Measurements. The magnetic circular dichroism (MCD) of a molecule is measured exposing the molecule to a magnetic field parallel (by convention, the direction of the magnetic field is north to south) with the light propagation axis and defined as the difference in absorption of left- and right-circularly polarized light.

$$MCD(\tilde{\nu}) = A_l(\tilde{\nu}) - A_r(\tilde{\nu}) \quad (8)$$

The MCD of KtC was measured in phosphate buffer (pH 7.5) using a Jasco J-720 CD spectropolarimeter equipped with a permanent horseshoe magnet. The spectra were recorded with both NS (north-south) and SN magnetic field orientation. The MCD was obtained by subtracting the SN spectrum from the NS spectrum and dividing by 2. The MCD signal of $CoSO_4$ ($\Delta\epsilon_{19600\ cm^{-1}} = -0.0188\ M^{-1}\ cm^{-1}\ T^{-1}$) was used as a reference to calibrate the magnetic field.[39,40]

Quantum Chemical Calculations. Molecular orbital calculations of electronic absorption spectra were performed with the semiempirical ZINDO/S method as incorporated in the HyperChem program.[41] All singly excited configurations using the 15 highest occupied and 15 lowest unoccupied orbitals were included in the configuration interaction (CI). The geometries used were obtained from AM1 calculations as implemented in HyperChem.

The geometry of neutral tC was also optimized using density functional theory (DFT) with the B3LYP hybrid functional[42,43] and the 6-31G** basis set.[44] Calculation of the vibrational spectrum confirmed that the optimized structure corresponds to a minimum on the potential energy surface. The Gaussian 98 program package was used for these calculations.[45]

Results

Effects of pH on Absorption and Fluorescence Spectra. Figure 2 shows isotropic absorption spectra of the potassium salt of 1,3-diaza-2-oxophenothiazin-3-yl[32] acetic acid (KtC) at various pH values. In Figure 2a and b, the equilibrium between tC and its protonated and deprotonated form, respectively, is followed. The arrows in Figure 2a show the spectral evolution as the pH decreases, whereas in Figure 2b, arrows refer to increase in pH. From these results, it is obvious that the neutral form of tC has its lowest energy band maximum at 375 nm (26 700 cm^{-1}). Moreover, no significant change can be seen between the spectra recorded at pH 7.5 and 4.0 (top two spectra at 26 700 cm^{-1}, Figure 2a) or between pH 7.5 and 12.0 (lowest two spectra at 26 700 cm^{-1}, Figure 2b), indicating that this neutral form of tC is predominant in the pH interval 4−12.

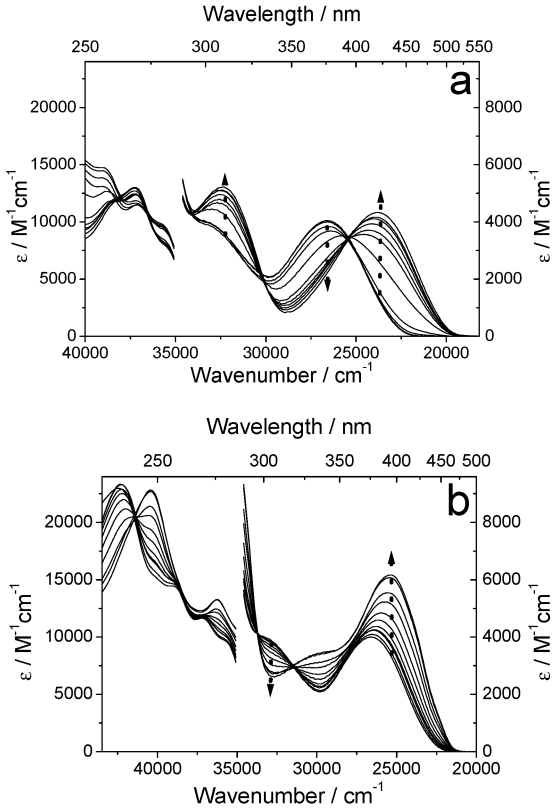

Figure 2. Isotropic absorption spectra (A_{iso}) of pH titration of tC. pH titration ranging from −0.5−7.5 (a), where the arrows indicate decrease in pH (pH = 7.5, 4.0, 3.0, 2.0, 1.0, 0.4, 0.2, 0, −0.1, −0.3, and −0.5). A citrate buffer (50 mM Na^+) with addition of HCl was used, except at pH 7.5, where a phosphate buffer (50 mM Na^+) was used. pH titration ranging from 7.5 to 14 (b), where the arrows indicate increase in pH (pH = 7.5, 12.0, 12.4, 12.6, 12.8, 13.0, 13.2, 13.4, 13.6, 13.8, and 14). A glycine−NaOH buffer (50 mM Na^+) with addition of NaOH was used, except at pH 7.5, where a phosphate buffer (50 mM Na^+) was used. The extinction coefficients for the wavenumbers below 35 000 cm^{-1} are given on the right-hand *y* axis. Measurements performed at 25 °C.

TABLE 1: Wavenumber Maxima ($\tilde{\nu}_{max}$) and Extinction Coefficient Maxima (ϵ_{max}) of the Lowest Energy Absorption Band and Fluorescence Quantum Yield (ϕ_f) of tC Nucleoside in Buffer Solution at Different pHs

	$\tilde{\nu}_{max}/cm^{-1}$	$\epsilon_{max}/M^{-1}\ cm^{-1}$	ϕ_f[a]
pH −0.5	23 800	4300	<0.01
pH 4	26 700	4000	0.16
pH 7.5	26 700	4000	0.17
pH 10	26 700	4000	0.17
pH 14	25 400	6200	0.11

[a] Fluorescence quantum yield measured relative to the quantum yield of 9,10-diphenylanthracene in ethanol ($\phi_f = 0.95$).[37]

However, lowering the pH, a protonated form of tC with an absorption maximum at ~23 800 cm^{-1} appears (Figure 2a). An estimation of pK_a for the equilibrium between the protonated and the neutral forms of tC gives 1.0 ± 0.2, when instead, raising the pH, a deprotonated form of tC having an absorption maximum at 25 400 cm^{-1} emerges (Figure 2b). An estimation of pK_a for the equilibrium between the neutral and the deprotonated forms of tC gives 13.2 ± 0.2.

Table 1 summarizes the observations from Figure 2 concerning the absorption maximum of the lowest energy transition and the estimated extinction coefficients belonging to this transition for tC at varying pH (for extinction coefficient determination, see Materials and Methods). It should be noted

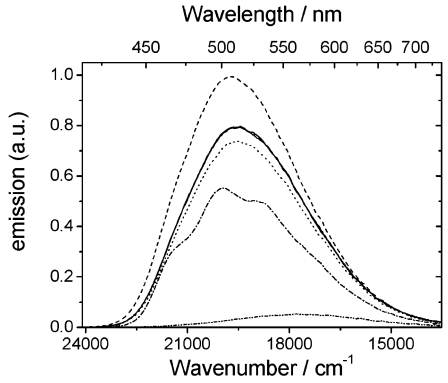

Figure 3. Emission spectra of the tC nucleoside at different pHs. Included for comparison is the emission spectrum of KtC at pH 7.5 (− −). Emission of the tC nucleoside at pH 7.5 and 10 (—), 4 (·····), 14 (−·−), and −0.5 (−··). The buffers used were the same as in the legend of Figure 2. Measurements performed at 25 °C.

TABLE 2: Wavenumber Maxima ($\tilde{\nu}_{max}$) and Extinction Coefficient Maxima (ϵ_{max}) of the Lowest Energy Absorption Band and Fluorescence Quantum Yields (ϕ_f) of tC in Different Solvents

	$\tilde{\nu}_{max}$/cm^{-1}	ϵ_{max}/M^{-1} cm^{-1}	ϕ_f[a]
buffer[b]	26 700	4000	0.20
ethanol[c]	26 900	3900	0.46
chloroform	26 700	3600	0.57
acetonitrile[d]	27 100	3500	0.47
THF[d]	27 000	3100	0.49

[a] Fluorescence quantum yield measured relative to the quantum yield of 9,10-diphenylanthracene in ethanol ($\phi_f = 0.95$).[37] [b] KtC form of tC in a phosphate buffer (50 mM Na^+, pH 7.5). [c] AtC form of tC was used. [d] MtC form of tC was used.

that both the protonated and deprotonated forms of tC, besides being considerably red-shifted as compared to the neutral form (vide supra), also have extinction coefficients that are significantly higher.

Table 1 also shows the fluorescence quantum yield of the tC nucleoside at different pH values. The emission profiles belonging to the quantum yield values in Table 1 can be seen in Figure 3, where they are compared to the normalized emission of KtC. The emission maxima of the tC nucleoside at pH 4, 7.5, and 10 coincides at ∼19 600 cm^{-1} but are slightly red-shifted compared to KtC (Em_{max} = 19 800 cm^{-1}). Furthermore, the emission is weaker for the neutral form of the tC nucleoside (ϕ_f = 0.16−0.17) than for the corresponding form of KtC (ϕ_f = 0.20). At low pH, where the protonated form of the tC nucleoside is predominant, the emission is substantially red-shifted (Em_{max} ∼ 17 700 cm^{-1}) compared to the neutral form, and the quantum yield (ϕ_f < 0.01) is considerably lowered. Also at high pH, the quantum yield of the tC nucleoside (ϕ_f = 0.11) is lower than at neutral pH, but the drop is by no means as large as at low pH. It can also be noted that the emission profile for the deprotonated form of the tC nucleoside is structured and has its maximum at ∼20 000 cm^{-1}.

Solvent Effects on Photophysical Properties. Table 2 shows the wavenumber maxima ($\tilde{\nu}_{max}$) and the extinction coefficient maxima (ϵ_{max}) of the lowest energy absorption band and the fluorescence quantum yields (ϕ_f) of tC in different solvents.

The Table shows that the influence of solvent on the wavenumber maximum of the lowest energy absorption band, ranging from 26 700 cm^{-1} in phosphate buffer to 27 100 cm^{-1} in acetonitrile, is small. The extinction coefficient maxima show some differences between solvents, ranging from 4000 M^{-1} cm^{-1} in phosphate buffer to 3100 M^{-1} cm^{-1} in THF. However,

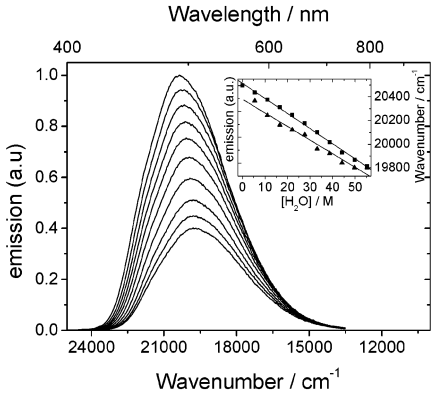

Figure 4. Emission spectra of KtC at water/ethanol ratios ranging from 10:0 to 1:9. Measurements were performed at 25 °C. Inset: Linear fits of emission intensities (■) and wavenumbers at emission maxima (▲) as a function of water concentration.

the most significant variations can be observed by comparing the fluorescence quantum yields. In ethanol, chloroform, acetonitrile, and THF, the quantum yields are on the order of 50%, whereas in buffer, it is only 20%. Moreover, the emission profile of tC in buffer is more red-shifted (Em_{max} = 19 800 cm^{-1}, Figure 3) than in any other of the solvents (Em_{max} ranging from 21 300 to 20 400 cm^{-1}, data not shown).

Figure 4 shows a titration of water into an ethanol solution of KtC. The emission spectra are measured with an interval of 10%, ranging from 90 (top spectrum) to 0% (bottom spectrum) ethanol. It can clearly be observed that the emission decreases with addition of water. In addition, as mentioned above, a small red shift can be observed when increasing the concentration of water. The inset shows that a virtually linear relationship can describe the dependence of both fluorescence intensity and wavenumber shift at emission maximums as a function of increasing water concentration.

Polarized Light Spectroscopy. Figure 5a shows the isotropic absorption spectrum, reduced linear dichroism (LD^r), and the fluorescence anisotropy of tC. The fluorescence anisotropy over the lowest energy absorption band nearly reaches the theoretical maximum value for anisotropy (∼0.4), showing that the excited molecules are practically totally immobilized on the time scale of excited state deactivation. Moreover, this anisotropy indicates, as expected, that the absorbing and emitting transition moments are parallel. It should also be observed that the anisotropy is essentially constant over the lowest energy band (22 300−30 000 cm^{-1}), signifying the same orientation of transition moment(s) in the whole region, indicating that this band originates from a single absorbing transition moment. At 33 300 cm^{-1}, a dip in anisotropy indicates the presence of a second transition that is polarized at least 30° relative to the lowest energy transition. The positive LD^r over the absorption band centered at 26 700 cm^{-1} shows a significant slope, which may appear to be in conflict with a pure polarization of a single electronic transition of this band, which observation we shall return to in the Discussion.

Figure 5b shows the magnetic circular dichroism (MCD) of the lowest energy absorption band of KtC. For two electronic transitions close in energy with transition moments that are not parallel with each other, the magnetic field will mix the two electronic states involved, leading to magnetic rotational strengths of opposite signs but equal in amplitudes. Therefore, a MCD spectrum will be bisignate in such a case and, thus, can be used to discern whether an absorption band consists of one or several transitions. The lack of change in signs over the lowest energy absorption band and the similarity between the

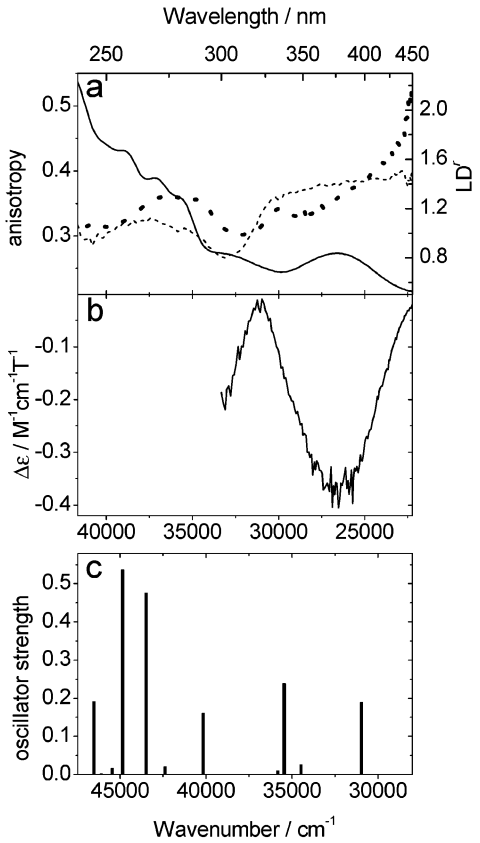

Figure 5. (a) Isotropic absorption spectrum (A_{iso}, —), reduced linear dichroism (LD^r, ·····), and excitation anisotropy (r, — —) of KtC. A_{iso} was measured in a phosphate buffer (50 mM Na^+, pH 7.5); LD^r, in a stretched PVA film; and r, in a H_2O/1,2-etandiol (1:2 mixture) glass at −100 °C. (b) Magnetic circular dichroism (MCD) of KtC in phosphate buffer (50 mM Na^+, pH 7.5). (c) Calculated electronic transitions of the tC chromophore and their oscillator strengths. Energy optimization of molecular geometry was performed using the semiempirical method AM1. Electronic excitation spectrum was calculated using the semiempirical method ZINDO/S. Fifteen occupied and 15 unoccupied orbitals were included in the configuration interaction (CI). Note that the wavenumber scale in part c is displaced compared to parts a and b.

MCD spectral profile and the absorption spectrum suggests that the first absorption band is due to only a single electronic transition. This is in agreement with the anisotropy results (vide supra) that one single transition gives rise to the lowest absorption band between 22 300 and 30 000 cm^{-1}.

Molecular Orbital Calculations—Structures and Spectra. The geometry of the neutral tC base is predicted from both the AM1 and the DFT B3LYP/6-31G** calculations to be folded along the middle ring sulfur−nitrogen axis with a dihedral angle of ∼170−155° (See Supporting Information for AM1 coordinates). Because the calculated AM1 and DFT B3LYP/6-31G** geometries have no significant differences, we arbitrarily choose the AM1 structure for further calculation of electronic spectra. The result from the calculated structure is in good agreement with the X-ray crystal structure of the parent molecule phenothiazine.[46,47] The protonated form is also predicted (AM1) to have a folded structure, whereas the optimized geometry of the deprotonated form shows no significant deviations from planarity.

In Figure 5c, the electronic spectrum of the neutral form of tC (AM1 geometry), calculated using ZINDO/S, is shown for comparison with the measured spectra. To facilitate comparison, the wavenumber scale of the calculated spectrum is displaced by 5800 cm^{-1} compared to the spectra in Figure 5a and b. In Table 3, the details for the strongest transitions of the neutral form of tC below 46 550 cm^{-1} are given, together with the corresponding results for the protonated and deprotonated forms. We shall return to the details of the calculated spectra in the Discussion.

Discussion

A very promising, although not unexpected, result in this study is the fact that the 2-deoxyribonucleoside of 1,3-diaza-2-oxophenothiazine has basically the same fluorescence quantum yield ($\phi_f = 0.17$) as the 1,3-diaza-2-oxophenothiazin-3-yl acetic acid (AtC) ($\phi_f = 0.20$) in aqueous buffers at neutral pH.[33] Previously, we have shown that synthesis of a PNA monomer of AtC and subsequent incorporation into a single-stranded PNA left the fluorescence quantum yield essentially unchanged ($\phi_f = 0.22$). Furthermore, upon hybridization to a complementary single-stranded DNA, the fluorescence quantum yield of the tC base in the PNA strand was found to be preserved (ϕ_f,= 0.21). This suggests that the fluorescence quantum yield, also upon incorporation of the 2-deoxyribonucleoside of 1,3-diaza-2-oxophenothiazine into a single-stranded DNA and subsequent hybridization to a complementary DNA strand (work currently in progress), will be high and essentially independent of context. In light of this promising result and to facilitate future biophysical studies, using tC as a fluorescent base analogue, we will discuss the basic photophysical properties of the DNA base analogue below.

Absorptive and Emissive Properties at pH Extremes. As can be seen in Figure 2, both the protonated and deprotonated forms of tC have their lowest energy transition at lower wavenumbers, ∼23 800 and 25 400 cm^{-1}, respectively. In addition, the extinction coefficients of these two transitions are larger than for the neutral form (Table 1). It should be noted that the molecular orbital calculations on both the protonated (proton on N1) and deprotonated forms of tC (Table 3) result in red shifts and increases in extinction coefficients relative the neutral form, albeit not all details are accurately predicted. Furthermore, the calculations suggest that the lowest energy transitions for the protonated and deprotonated forms are largely long-axis-oriented (z, in Figure 1), in good agreement with the experimental results.

The fluorescence quantum yield of the protonated form ($\phi_f < 0.01$) is appreciably lowered, and there is also a red shift in emission as compared to the neutral form of tC. In addition, for the deprotonated form, which interestingly has a structured emission profile, a decrease in quantum yield can be observed ($\phi_f = 0.11$). The structured emission profile of the deprotonated form might come as a result of a planar, more rigid structure, which is also supported by the quantum chemical calculations.

Absorptive and Emissive Properties at Neutral pH. A consequence of the pK_a values for the equilibria between the neutral and both the protonated (pK_a = 1.0 ± 0.2) and the deprotonated form (pK_a = 13.2 ± 0.2) of tC is that there are extremely low amounts of these forms at neutral pH. The neutral form of tC is, as mentioned above, predominant in the pH interval 4−12. The lowest energy transition of the tC nucleoside has, like AtC, its maximum at 26 700 cm^{-1} (Table 1). Moreover, the fluorescence quantum yield of the tC nucleoside in its neutral form is 0.17 (Table 1). A small decrease can be observed for the emission measured at pH 4 (Figure 3 and Table 1). However, because only 0.1% of tC is in its protonated form at pH 4, it seems highly unlikely that the decrease in fluorescence quantum yield compared to the one obtained at pH 7.5 (Table 1) would come as a result of the equilibrium between the protonated and

TABLE 3: Strongest Calculated Electronic Transitions[a] below 46 550 cm^{-1} for Deprotonated tC, tC, and Protonated tC Calculated Using ZINDO/S[b]

deprotonated tC				tC				protonated tC			
trans	$\tilde{\nu}$/cm^{-1}	f[c]	δ[d]/deg	trans	$\tilde{\nu}$/cm^{-1}	f[c]	δ[d]/deg	trans	$\tilde{\nu}$/cm^{-1}	f[c]	δ[d]/deg
$S_0 \rightarrow S_1$	28 500	0.773	5	$S_0 \rightarrow S_1$	31 000	0.190	−36	$S_0 \rightarrow S_1$	22 500	0.235	−17
$S_0 \rightarrow S_2$	30 900	0.079	−52	$S_0 \rightarrow S_4$	35 500	0.238	37	$S_0 \rightarrow S_2$	30 400	0.087	−5
$S_0 \rightarrow S_6$	36 500	0.056	40	$S_0 \rightarrow S_6$	40 200	0.160	−21	$S_0 \rightarrow S_4$	32 800	0.106	−71
$S_0 \rightarrow S_8$	40 800	0.095	74	$S_0 \rightarrow S_8$	43 500	0.476	29	$S_0 \rightarrow S_6$	37 000	0.165	5
$S_0 \rightarrow S_{12}$	43 700	0.803	−18	$S_0 \rightarrow S_9$	44 800	0.536	−16	$S_0 \rightarrow S_8$	43 300	0.198	84
$S_0 \rightarrow S_{14}$	45 700	0.322	37	$S_0 \rightarrow S_{12}$	46 500	0.192	14	$S_0 \rightarrow S_{12}$	46 300	0.466	2

[a] Cutoffs of oscillator strengths for deprotonated tC, tC, and protonated tC are 0.024, 0.026, and 0.051, respectively. [b] 451 singly excited configurations were included in the CI calculation. [c] Oscillator strength. [d] In-plane angle relative the long axis (z) of the molecule, as defined in Figure 1.[48]

neutral forms of tC. Instead, this most certainly comes as a result of the pK_a of the excited state not being the same as the pK_a of the ground state.

Emissive Properties in Different Solvents. The fluorescence quantum yields in all the examined solvents, except in buffer (0.20), are on the order of 0.5 (Table 2). Previously, we have found that the quantum yield of tC upon incorporation into a single-stranded PNA (0.22) or into a DNA−PNA duplex (0.21) is essentially unchanged, as compared to the free form.[33] Thus, the less polar environment that comes as a result of incorporating tC into oligonucleotides or when changing from water to less polar solvents affects the fluorescence quantum yield in different ways. Instead, we suggest that hydrogen bonding to tC might play an important role in lowering the quantum yield. When tC exists in its free form in buffer or when it is incorporated into a single-stranded PNA, still in buffer solution, hydrogen bonding between water and tC is possible. Obviously, tC is also involved in hydrogen bonding when it is incorporated into a PNA, and the latter is hybridized to a complementary DNA. The other solvents, ethanol included, will be less suited for hydrogen bonding than water or a guanine in a complementary DNA strand, which might explain the increase in quantum yields by a factor of ∼2.5.

Spectral Details for the Neutral Form of tC. The isotropic absorption spectrum in Figure 5a shows that the lowest energy absorption band for tC in its neutral form has a wavenumber range from 22 300 to 30 000 cm^{-1}. To facilitate future accurate distance measurements using FRET, we need to answer the question whether the lowest energy absorption band consists of one or more electronic transitions as well as the polarization of their transition moments. As mentioned, the constant anisotropy over this band leaves only two alternatives, namely, that there is only one transition in this wavenumber range or that there are several transitions with the same transition moment directions. The fluorescence anisotropy value further indicates that they have to be the same as that of the emitting transition moment. Additionally, the purely negative MCD in Figure 5b further supports a conclusion that the lowest absorption energy band consists of only one electronic transition, although it cannot exclude the possibility of two transitions with the same transition moment directions. To further examine the credibility of a single electronic transition giving rise to the lowest energy absorption band, we have applied the Strickler−Berg equation[49] to our experimental data,

$$\frac{1}{\tau_0} = 2.880 \times 10^{-9} n^2 \langle \tilde{\nu}_f^{-3} \rangle^{-1} \left(\frac{g_l}{g_u}\right) \int \epsilon(\tilde{\nu})\, \mathrm{d} \ln \tilde{\nu} \qquad (9)$$

where n is the refractive index of the solvent, $\langle \tilde{\nu}_f^{-3} \rangle^{-1}$ is the reciprocal of the mean value of $\tilde{\nu}^{-3}$ in the fluorescence spectrum, g_l and g_u are the degeneracies of the lower and upper states, respectively, and $\epsilon(\tilde{\nu})$ is the molar absorptivity at wavenumber $\tilde{\nu}$. The equation relates the theoretical (natural) lifetime (τ_0) to the absorption intensity (area under the absorption band corresponding to the $S_0 \rightarrow S_1$ transition). Using the Strickler−Berg equation gives a calculated value for τ_0 of 32.5 ns. The measured natural lifetime, τ_0, is related to the measured lifetime, τ, by the fluorescence quantum yield: $\tau = \tau_0 \phi_f$. The observed lifetime and fluorescence quantum yield for tC are 3.7 ns and 0.20, respectively.[33] This gives a natural lifetime of 18.5 ns. Although the calculated natural lifetime is longer than the measured one, it is still reasonable to conclude, on the basis of the anisotropy and MCD, that the lowest energy absorption band consists of only a single electronic transition.

By contrast, the sloping LD^r over this band, at first glance, suggests quite the opposite. However, from isotropic absorption of KtC in buffer, we know that the spectrum is red-shifted, upon considerable increase in concentration, suggesting aggregation, maybe a dimerization, of the hydrophobic ring systems. The high concentration of tC in the dried PVA films (∼2 mM) most likely pushes the equilibrium toward aggregation, giving a mixture between tC monomers and aggregates. Thus, there will be a mixture between two different absorbing species in the region between 30 300 and 22 200 cm^{-1}. The slope, therefore, might come as a result of the two species having different degrees of orientation in the PVA film and/or that their transition moment directions relative to the molecular orientation axis are different. This mixture of species unfortunately makes a quantitative assignment of the transition moment directions of the tC chromophore, from LD^r measurements, more difficult.

To estimate the orientation of tC in the PVA matrix, we use the fact that tC is structurally comparable to the DNA intercalator methylene blue. Previously, it has been concluded that methylene blue orients nearly like a rodlike molecule in PVA matrices.[50] Further support of a rodlike orientation of tC is that the spectral profiles of the anisotropy and the LD^r would then be basically similar (eqs 2, 3 and 6, 7), as is, indeed, found here. Thus, once we know the orientation parameter, S_{zz}, we can use eq 7 to estimate the angle, θ_i, between the electronic transition moments and the molecular orientation axis. Earlier, the principal orientation parameter, S_{zz}, has been found to be ∼0.78 for methylene blue.[50] A good estimate of the LD^r of the lowest energy transition of the tC monomer is obtained using the value at the absorption maximum (26 700 cm^{-1}), namely, LD^r = 1.27. This LD^r value for the tC monomer and the S_{zz} adopted from methylene blue gives an angle between the lowest electronic transition moment and the molecular orientation axis, z, of 34°. Furthermore, it is expected that the molecular orientation axis essentially coincides with the long-axis of tC (z, in Figure 1), suggesting that the lowest electronic transition has an angle of ∼35° relative to this axis.

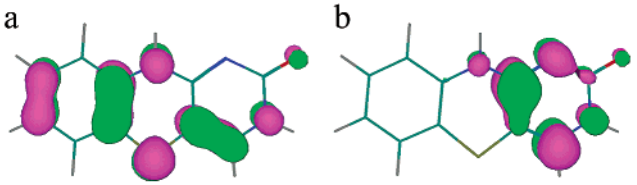

Figure 6. (a) Highest occupied molecular orbital (HOMO) and (b) lowest unoccupied molecular orbital (LUMO) of tC with an isosurface value of 0.05.

The quantum chemical calculations give an angle between the long axis in tC, *z*, and the $S_0 \rightarrow S_1$ transition of −36° (as defined in Figure 1 and Table 3), in excellent agreement with experiment. This transition is mainly a HOMO−LUMO transition (CI coefficient 0.92) with considerable charge transfer character. This charge transfer character originates from the fact that the coefficients of the N1 nitrogen, C2 carbon, and the carbon between N10 and N1 of the HOMO are essentially zero (Figure 6a), whereas the LUMO is characterized by very low coefficients on the benzene ring (Figure 6b), thus giving rise to a substantial redistribution of charges. The ground state dipole moment is 7.02 D, having approximately the same direction as the axis joining N1 and C6, whereas the dipole moment of the first excited state is 10.7 D, with approximately the same direction as the ground-state dipole moment.

The first dip in anisotropy, going from low wavenumbers (Figure 5a), suggests that the second lowest absorption band has its low energy tail at ∼30 000 cm^{-1}. As mentioned above, the minimum at 33 300 cm^{-1} indicates a transition that is directed 30° relative the lowest energy transition. However, considering the overlap with transitions, mainly of higher energy, and the observation that the LD^r at 33 300 cm^{-1} is lower than at 26 700 cm^{-1}, it is highly likely that the angle between this transition and the lowest energy transition is considerably more than 30°. The molecular orbital calculations predict that the transition second-lowest in energy with significant oscillator strength ($\tilde{\nu}$ = 35500 cm^{-1}, f = 0.238) is directed +37° (as defined in Figure 1 and Table 3) relative the molecular long axis, *z*, thus in good agreement with both the anisotropy and LD^r. At even higher energies, the transition moment overlap is severe, but the anisotropy, LD^r, and quantum chemical calculations all indicate that the third transition with significant intensity has an orientation that is closer to the lowest energy transition and also the molecular orientation axis, *z*.

Conclusions

The following has been learned from this photophysical characterization of the novel fluorescent DNA base analogue, tC:

1. The neutral form of tC, that is, the one being able to form Watson−Crick base pairs, is the totally predominant form in a large pH interval, 4−12. It is characterized by strong fluorescence, virtually invariant of nucleobase environment, and therefore, suitable for use as a biophysical probe of molecular dynamics and distance geometry.

2. The lowest energy absorption, centered at 26 700 cm^{-1}, is well separated from the absorption of the nucleobases and has a transition moment polarized at an angle of ∼35° to the long axis of the tC chromophore.

Acknowledgment. This project was funded by The Swedish Research Council (VR).

Supporting Information Available: Table of AM1 optimized structure of the neutral, base pairing form of 1,3-diaza-2-oxopheno-thiazine, tC. This material is available free of charge via the Internet at http://pubs.acs.org.

References and Notes

(1) Rist, M. J.; Marino, J. P. *Curr. Org. Chem.* **2002**, *6*, 775.
(2) Ward, D. C.; Reich, E.; Stryer, L. *J. Biol. Chem.* **1969**, *244*, 1228.
(3) Holmén, A.; Nordén, B.; Albinsson, B. *J. Am. Chem. Soc.* **1997**, *119*, 3114.
(4) Freese, E. *J. Mol. Biol.* **1959**, 87.
(5) Rachofsky, E. L.; Osman, R.; Ross, J. B. A. *Biochemistry* **2001**, *40*, 946.
(6) Guest, C. R.; Hochstrasser, R. A.; Sowers, L. C.; Millar, D. P. *Biochemistry* **1991**, *30*, 3271.
(7) Stivers, J. T. *Nucleic Acids Res.* **1998**, *26*, 3837.
(8) Baker, R. P.; Reha-Krantz, L. J. *Proc. Natl. Acad. Sci. U.S.A.* **1998**, *95*, 3507.
(9) Bloom, L. B.; Otto, M. R.; Beechem, J. M.; Goodman, M. F. *Biochemistry* **1993**, *32*, 11247.
(10) Goodman, M. F.; Fygenson, D. K. *Genetics* **1998**, *148*, 1475.
(11) Hochstrasser, R. A.; Carver, T. E.; Sowers, L. C.; Millar, D. P. *Biochemistry* **1994**, *33*, 11971.
(12) Lam, W. C.; Van der Schans, E. J. C.; Sowers, L. C.; Millar, D. P. *Biochemistry* **1999**, *38*, 2661.
(13) Petrauskene, O. V.; Schmidt, S.; Karyagina, A. S.; Nikolskaya, II.; Gromova, E. S.; Cech, D. *Nucleic Acids Res.* **1995**, *23*, 2192.
(14) Nordlund, T. M.; Andersson, S.; Nilsson, L.; Rigler, R.; Gräslund, A.; McLaughlin, L. W. *Biochemistry* **1989**, *28*, 9095.
(15) Lycksell, P. O.; Gräslund, A.; Claesens, F.; McLaughlin, L. W.; Larsson, U.; Rigler, R. *Nucleic Acids Res.* **1987**, *15*, 9011.
(16) Allan, B. W.; Reich, N. O. *Biochemistry* **1996**, *35*, 14757.
(17) Allan, B. W.; Beechem, J. M.; Lindstrom, W. M.; Reich, N. O. *J. Biol. Chem.* **1998**, *273*, 2368.
(18) Allan, B. W.; Reich, N. O.; Beechem, J. M. *Biochemistry* **1999**, *38*, 5308.
(19) Stivers, J. T.; Pankiewicz, K. W.; Watanabe, K. A. *Biochemistry* **1999**, *38*, 952.
(20) Hawkins, M. E. *Cell Biochem. Biophys.* **2001**, *34*, 257.
(21) Hawkins, M. E.; Pfleiderer, W.; Mazumder, A.; Pommier, Y. G.; Falls, F. M. *Nucleic Acids Res.* **1995**, *23*, 2872.
(22) Hawkins, M. E.; Pfleiderer, W.; Balis, F. M.; Porter, D.; Knutson, J. R. *Anal. Biochem.* **1997**, *244*, 86.
(23) Hawkins, M. E.; Pfleiderer, W.; Jungmann, O.; Balis, F. M. *Anal. Biochem.* **2001**, *298*, 231.
(24) Driscoll, S. L.; Hawkins, M. E.; Balis, F. M.; Pfleiderer, W.; Laws, W. R. *Biophys J.* **1997**, *73*, 3277.
(25) Godde, F.; Aupeix, K.; Moreau, S.; Toulmé, J. J. *Antisense Nucleic Acid Drug Dev.* **1998**, *8*, 469.
(26) Godde, F.; Toulmé, J. J.; Moreau, S. *Biochemistry* **1998**, *37*, 13765.
(27) Godde, F.; Toulmé, J. J.; Moreau, S. *Nucleic Acids Res.* **2000**, *28*, 2977.
(28) Ren, R. X. F.; Chaudhuri, N. C.; Paris, P. L.; Rumney, S.; Kool, E. T. *J. Am. Chem. Soc.* **1996**, *118*, 7671.
(29) Strassler, C.; Davis, N. E.; Kool, E. T. *Helv. Chim. Acta* **1999**, *82*, 2160.
(30) Paris, P. L.; Langenhan, J. M.; Kool, E. T. *Nucleic Acids Res.* **1998**, *26*, 3789.
(31) Matray, T. J.; Kool, E. T. *Nature* **1999**, *399*, 704.
(32) The base analogue has previously incorrectly been called 3,5-diaza-4-oxophenothiazine. The correct IUPAC name should be 1,3-diaza-2-oxophenothiazine.
(33) Wilhelmsson, L. M.; Holmen, A.; Lincoln, P.; Nielsen, P. E.; Nordén, B. *J. Am. Chem. Soc.* **2001**, *123*, 2434.
(34) Lin, K.; Jones, R. J.; Matteucci, M. *J. Am. Chem. Soc.* **1995**, *117*, 3873.
(35) Eldrup, A. B.; Nielsen, B. B.; Haaima, G.; Rasmussen, H.; Kastrup, J. S.; Christensen, C.; Nielsen, P. E. *Eur. J. Org. Chem.* **2001**, 1781.
(36) Roth, B.; Schloemer, L. *J. Am. Chem. Soc.* **1963**, *28*, 2659.
(37) Morris, J. V.; Mahaney, M. A.; Huber, J. R. *J. Phys. Chem.* **1976**, *80*, 969.
(38) Lakowicz, J. R. *Principles of Fluorescence Spectroscopy*; Plenum Press: New York, 1983.
(39) Nordén, B.; Håkansson, R.; Danielsson, S. *Chem. Scr.* **1977**, *11*, 52.
(40) McCaffery, A. J.; Stephens, P. J.; Schatz, P. N. *Inorg. Chem.* **1967**, *6*, 1614.
(41) Copyright 1999 Hypercube, Inc.
(42) Becke, A. D. *J. Chem. Phys.* **1993**, *98*, 1372; 5648.
(43) Lee, C.; Yang, W.; Parr. R. G. *Phys. Rev.* **1988**, *B27*, 785.
(44) Hariharan, P. C.; Pople, J. A. *Theor. Chim. Acta* **1973**, *28*, 213.

(45) Frisch, M. J.; Trucks, G. W.; Schlegel, H. B.; Scuseria, G. E.; Robb, M. A.; Cheeseman, J. R.; Zakrzewski, V. G.; Montgomery, J. A., Jr.; Stratmann, R. E.; Burant, J. C.; Dapprich, S.; Millam, J. M.; Daniels, A. D.;. Kudin, K. N.; Strain, M. C.; Farkas, O.; Tomasi, J.; Barone, V.; Cossi, M.; Cammi, R.; Mennucci, B.; Pomelli, C.; Adamo, C.; Clifford, S.; Ochterski, J.; Petersson, G. A.; Ayala, P. Y.; Cui, Q.; Morokuma, K.; Malick, D. K.; Rabuck, A. D.; Raghavachari, K.; Foresman, J. B.; Cioslowski, J.; Ortiz, J. V.; Baboul, A. G.; Stefanov, B. B.; Liu, G.; Liashenko, A.; Piskorz, P.; Komaromi, I.; Gomperts, R.; Martin, R. L.; Fox, D. J.; Keith, T.; Al-Laham, M. A.; Peng, C. Y.; Nanayakkara, A.; Gonzalez, C.; Challacombe, M.; Gill, P. M. W.; Johnson, B.; Chen, W.; Wong, M. W.; Andres, J. L.; Gonzalez, C.; Head-Gordon, M.; Replogle, E. S.; Pople, J. A. *Gaussian 98*, Revision A.7; Gaussian, Inc.: Pittsburgh, PA, 1998.

(46) Bell, J. D.; Blount, J. F.; Briscoe, O. V.; Freeman, H. C. *J. Chem. Soc., Chem. Commun.* **1968**, 1656.

(47) McDowell, J. J. H. *Acta Crystallogr., B* **1976**, *32*, 5.

(48) The plane wherein *z* can be found is defined by carbon atoms C2, C7, and C8.

(49) Strickler, S. J.; Berg, R. A. *J. Chem. Phys.* **1962**, *37*, 814.

(50) Nordén, B. *J. Chem. Phys.* **1980**, *72*, 5032.